First. publ. in: Materials science - Poland 26 (2008), 4, pp. 983-988

Modelling of magnetization reversal for long ferromagnetic nanotubes

K. M. LEBECKI*

Institute of Physics, Polish Academy of Sciences, al. Lotników 32/46, 02-668 Warsaw, Poland

The theory of infinite tube magnetization reversal, formulated by Lee and Chang, has been reconsidered. For this purpose, a standard micromagnetic simulation package OOMMF was used. To account for elongated geometry of ferromagnetic nanotubes grown nowadays, an extension module has been written allowing application of periodic boundary conditions in one dimension. The results of the modelling exhibit a basic agreement with the theory. Limitations of the approach have been described and checkpoints have been discussed necessary in finite difference simulations performed for such structures.

Key words: *magnetic nanowires; micromagnetic modelling; magnetization reversal; coercivity*

1. Introduction

Self-assembly [1] as a cheap and reliable method to grow structured systems has been attracting interest for many years. Among samples intensively studied in recent years are ferromagnetic nanoobjects, due to their potential application in spintronic devices and interesting basic science phenomena. Such structures are often produced within porous matrix, and contain magnetic nanowires, see, e.g., review papers [2]. Beside nanowires, there are, however, already a few reports of successful growth of magnetic nanotubes, either hollow or filled with a semiconductor [3]. This situation opens a novel possibility to build hybrid ferromagnetic–semiconductor systems. When considering such structures, a question arises what are the magnetization properties of a long ferromagnetic tube itself. To answer this question we re-evaluate the theory of infinite tube magnetization and compare it with micromagnetic modelling. We highlight the necessary checkpoints that should be monitored during simulation of such structures.

*E-mail: lebecki@ifpan.edu.pl

2. Analytical theory

Analytical theory for both an infinite rod [4, 5] and for an infinite tube [6] predicts rectangular hysteresis loops with two possible reversal modes: *curling* and *buckling*. Additionally, a third mode, referred to as *coherent*, is also mentioned in this context. All these modes are schematically shown in Fig. 1.

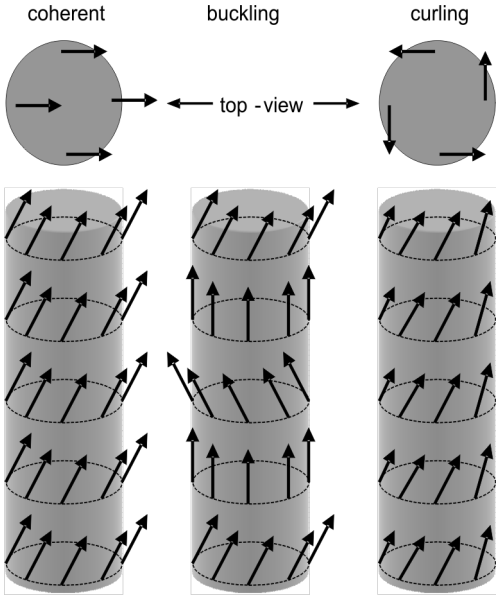

Fig. 1. Scheme of three reversal modes: coherent, buckling and curling. The arrows represent magnetization direction. The difference between coherent and curling modes can be seen from the top view presented above. A buckling mode exhibits periodicity along the tube axis

Coherent mode represents an in-unison reversal, where magnetization is uniform inside the sample. Buckling mode is similar to the coherent one, the magnetization is also uniform for any plane perpendicular to the tube axis but there additionally exists a periodicity of the magnetization distribution along the tube axis. The curling mode profile does not depend on the position of the axis. Instead, there is a rotational character of the magnetization (vortex-like).

Following earlier papers [4–6] we use notations (SI units):

$$R_0 = \sqrt{\frac{4\pi A}{\mu_0 M_S^2}},\ r = r_{ext} = \frac{R_{ext}}{R_0}, \qquad h = \frac{2H}{M_S}, \qquad \varepsilon = \frac{R_{int}}{R_{ext}}$$

where A is the exchange constant, M_S is saturation magnetization, R_{ext} (R_{int}) is the external (internal) tube radius, H is the applied external magnetic field, parallel to the tube axis, and ε is the radius ratio determining the tube wall thickness. In this paper, normalized values are used: h as a magnetic field, and r as the (external) tube radius. For tubes with smaller radii, the buckling reversal mode is preferred (i.e., energy of such a mode is lower), while for tubes with larger radii the curling mode is favoured [6] – see lines representing the theory in Fig. 2. The buckling nucleation field

is close to the coherent mode's value, $h_{coh}(r) = 1$. According to Aharoni and Shtrikman [4], in the case of an infinite solid rod, the transition from buckling to curling is abrupt. Critical radius where this transition takes place (see the arrow in Fig. 2) depends on the tube wall thickness. The period length of the buckling mode (see Fig. 1) increases to infinity for $r \to 0$, thus the coherent mode can be regarded as a special case of the buckling mode.

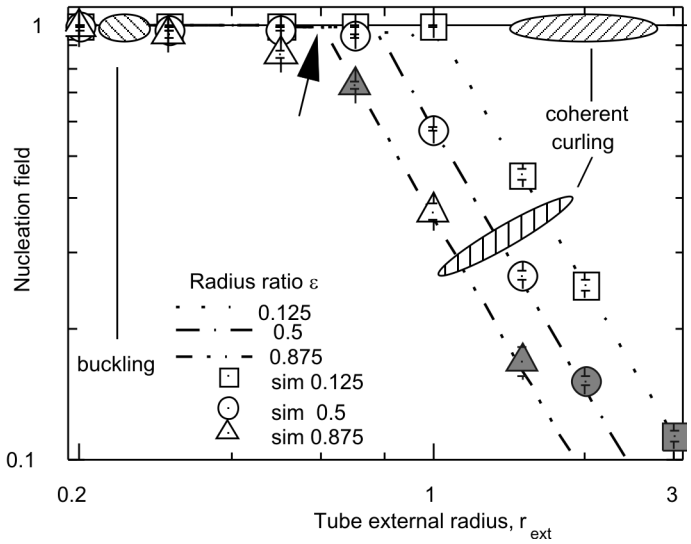

Fig. 2. Nucleation field for three nucleation modes. The lines represent the nucleation field as predicted by the theory [6]. The curves for three tube wall widths have been plotted. The buckling–curling transition, for $\varepsilon = 0.875$, is marked with an arrow. The dots represent results of our simulations. Gray-filled dots correspond to data not verified by the mesh density doubling process. See text for details

3. Computational details and simulation results

The nucleation field, predicted by the theory presented above, can be compared with the coercive field due to the rectangular shape of the hysteresis loops. In our modelling we used OOMMF micromagnetic software package [7]. A special module has been created [8] allowing one to include one-dimensional periodic boundary conditions (PBC) into the simulation. The PBC package takes into account exchange and magnetostatic interactions in numerically accurate way, see Ref. [9] for details. We used the following material parameters: $A = 9.604$ pJ/m, $M_S = 490$ kA/m (values resembling nickel), the anisotropy was neglected. These parameters lead to normalization values: $R_0 = 20$ nm, $(1/2)\mu_0 M_S \approx 308$ mT. As we have not been interested in any dynamic behaviour, we chose an energy minimalization algorithm. To verify our most intriguing results (Fig. 3), we also performed some tests using the dynamic algorithm

(damping coefficient was set to 0.5). These test data agreed with the energy minimization approach. The applied external magnetic field, parallel to the tube axis, was changed in steps with the step size dependent on the expected coercivity. The coercivity was calculated as the centre of the region where magnetization switching occurs, i.e., $H_C = |H_m + H_{m+1}|/2$, where H_m and H_{m+1} are consecutive applied fields, and $M(H_{m+1}) = -M(H_m)$. Such values are shown in Figs. 2 and 3 together with the error, defined as $\Delta H = |H_m - H_{m+1}|/2$. It is common in numerical simulations of hysteresis loops to apply an additional offset field to remove unintentional symmetry and to get stable results. Often this effect is introduced as a small tilt in the applied field direction. In our case, however, the symmetry had to be high, hence we had to employ another procedure. Namely, we applied a steady additional magnetic field with fixed magnitude, $\mu_0 H_{rnd} = 1$ mT, and with the direction chosen randomly for every cell in the sample. The magnitude of this field was chosen based on an analysis where we evaluated the hysteresis shape for different values of H_{rnd}. We found out that for small values of H_{rnd} the instabilities appear, while for large values the hysteresis start to change together with H_{rnd}. Around $\mu_0 H_{rnd} = 1$ mT, there exists a plateau where the results (like coercivity) essentially do not depend on H_{rnd}. In the case of the coherent and curling nucleation modes, due to their shape (Fig. 1), the magnetization is not dependent on the position along the tube axis. Thus, simulating these modes, it is sufficient to consider a small sample, one cell long along the tube axis, being the direction of applied periodic boundary conditions. We performed some test computations for longer samples and the resulting coercivity did not change.

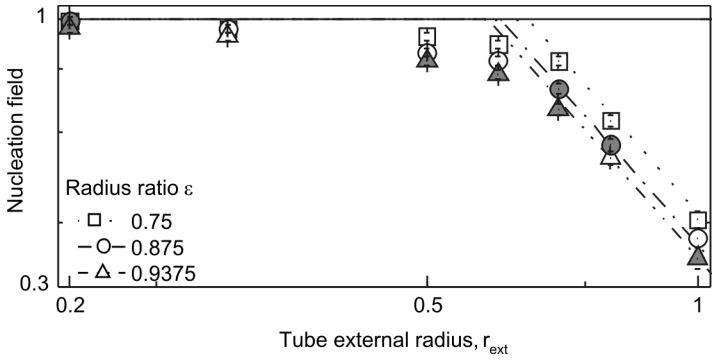

Fig. 3. Comparison between theoretical nucleation field and simulated coercivity for lager ε, and for smaller r

As our results appear to depend strongly on the cell size, we want to discuss this topic in more detail. In numerical simulations it is recommended to discretize the sample space into small enough cells, extending in every direction less than the magnetostatic exchange length, $\lambda_{ex} = R_0(2\pi)^{1/2}$, equal to ca. 8 nm in our case. In our simulations, we used cubic cells with the edge always shorter then 3 nm. Beside, however, the above-mentioned limit for the maximum cell size another issue must be taken into

account. Namely, the curved sample's surface may be a source of the so-called edge errors caused by the discretization process. To avoid this, one may introduce edge corrections either in a simplified way, by "diluting" the surface cells magnetization, or more precisely, by taking into account the complicated nature of demagnetization interactions for edge cells. But, as can be seen in Ref. [10], the simplified method, if used on its own, may actually increase the introduced errors. That is why we chose another solution: every our simulation was repeated for a twice denser mesh. If the resultant coercivity was within the abovementioned error, ΔH, we assumed that the mesh was dense enough. If not, the procedure was repeated. Almost all our results were verified according to this process, with a few exceptions explicitly noted.

Simulation results, together with the theoretical predictions are shown in Fig. 2 for three values of tube wall parameter, ε. Our records are limited by the constraint, described above, regarding "mesh density doubling" error checking. Due to this process, data for larger radii are not shown, as in that region they quickly start to differ, unless sufficiently dense mesh is used. In Figures 2 and 3 we show a few supplementary results, which were not verified by the mesh density doubling process; we mark them as gray-filled dots. From Figure 2, one can see a discrepancy between the theory and the modelling for larger ε in the region $r < 1$ (the simulation result for $r = 1$ and $\varepsilon = 0.125$ will be discussed separately in the next section). To investigate it further we made additional simulations for a smaller tube wall thickness. Relevant data can be found in Fig. 3.

4. Discussion and conclusions

Our modelling agrees with the theory of Lee and Chang [6] over a comparatively large range of parameters. The discrepancy between the simulated coercivity for $r = 1$ and $\varepsilon = 0.125$ (Fig. 2) on the one side, and the theory of buckling mode the other, can be explained by the fact that chosen length of our simulation samples permits a comparison with coherent or curling mode *only*. To take into account the buckling mode, one would have to make a simulation for the sample length, i.e., PBC period segment, being with agreement with the period length predicted for the buckling mode (see Fig. 1). Such an analysis has been done by us for a solid infinite rod [9], see also appropriate picture in Ref. [8]. Thus, selecting proper sample length would most probably eliminate this effect.

The disagreement between the theory and simulations present for thinner tube walls, visible in Fig. 3, cannot be explained in this way, for obvious reasons. In this radius range, the difference between the nucleation fields for coherent and buckling mode is already very small, as compared to the observed data discrepancy. Although not all points in this figure are verified by the mesh density doubling process, the tendency that the modelled coercivity is smaller, compared to the theory, is rather apparent here. The authors of the theory are unable to describe this difference [11]. A poten-

tial explanation could be a smooth transition from the coherent mode to a curling one for tubes with larger ε, a possibility somehow inconsistent with the abrupt transition buckling-curling mentioned by Aharoni and Shtrikman in Ref. [4].

The theory of infinite tube agrees well with simulations over a wide range of parameters. Small differences are present for thinner tube walls ($\varepsilon \geq 0.5$) in the proximity of buckling-curling transition, where the simulated coercivity is smaller than the theoretical prediction of the nucleation field. Reliable modelling requires a careful checking for the existence of possible edge errors and removal of unwanted symmetry, which in case of PBC simulations may be not as trivial, as without them.

Acknowledgements

The author acknowledges the proof reading of the manuscript by M.W. Gutowski.

References

[1] WHITESIDES G.M., GRZYBOWSKI B., Science, 295 (2002), 2418.
[2] SELLMYER D.J., ZHENG M., SKOMSKI R., J. Phys.: Condens. Matter, 13 (2001), R433; LI S., YAOWU H., CHIA-LING C., PETER C.S., IBM J. Res. Dev., 49 (2005), 79.
[3] KAZAKOVA O., DALY B., HOLMES J.D., Phys. Rev. B, 74 (2006), 184413; NIELSCH K., CASTANO F.J., ROSS C.A., KRISHNAN R., J. Appl. Phys., 98 (2005), 34318; CROWLEY T.A., DALY B., MORRIS M.A., ERTS D., KAZAKOVA O., BOLAND J.J., WU B., HOLMES J.D., J. Mater. Chem., 15 (2005), 2408.
[4] AHARONI A., SHTRIKMAN S., Phys. Rev., 109 (1958), 1522.
[5] FREI E.H., SHTRIKMAN S., TREVES D., Phys. Rev., 106 (1957), 446.
[6] LEE C.M., CHANG C.R., Mater. Chem. Phys., 43 (1996), 183; CHANG C.R., LEE C.M., YANG J.S., Phys. Rev. B, 50 (1994), 6461.
[7] DONAHUE M.J., PORTER D.G., OOMMF User's Guide, Version 1.0, Report NISTIR 6376, National Institute of Standards and Technology, Gaithersburg, MD, U.S.A., (1999). See: http://math.nist.gov/oommf.
[8] LEBECKI K.M., http://info.ifpan.edu.pl/~lebecki/pbc.htm.
[9] LEBECKI K.M., DONAHUE M.J., GUTOWSKI M.W., J. Phys. D: Appl. Phys., 41 (2008), 175005.
[10] DONAHUE M.J., MCMICHAEL R.D., IEEE Trans. Magn., 43 (2007), 2878.
[11] CHANG C.R., private communication, 2006.

Received 7 May 2007
Revised 22 September 2007